



## Analyzing Stability and Controlling Chaos in a Unique Host Parasitoid Discrete Dynamical System with Applications in Artificial Intelligence

Shaymaa H. Salih<sup>1</sup>, Nadia M.G. Al-Saidi<sup>1</sup>, Azhar Malik<sup>2</sup>, Suzan J. Obaiys<sup>3\*</sup>

<sup>1</sup> Department of Applied Sciences, University of Technology, Baghdad 110066, Iraq

<sup>2</sup> Department of Computer Engineering, University of Technology, Baghdad 110066, Iraq

<sup>3</sup> Computer Science and Information Technology, University Malaya, Kuala Lumpur 50603, Malaysia

Corresponding Author Email: [suzan@um.edu.my](mailto:suzan@um.edu.my)

Copyright: ©2024 The authors. This article is published by IETA and is licensed under the CC BY 4.0 license (<http://creativecommons.org/licenses/by/4.0/>).

<https://doi.org/10.18280/mmep.110817>

### ABSTRACT

**Received:** 2 December 2023

**Revised:** 16 April 2024

**Accepted:** 25 May 2024

**Available online:** 28 August 2024

#### Keywords:

Host-Parasitoid, stability, chaos, control, stabilization, artificial intelligence

This paper examines the specifics of studying the dynamics of the behavior of the host and the parasitoid in two dynamic systems. The host model HPM is an extension to a 2D system, where an arctan function acts as an activation function. It was chosen because it can be used in artificial neural networks of intelligence. Thus, the modeling process leads to the following representation of the essence of this model: the population dynamics in the main plane occur over discrete time intervals and by several formulae. These equations were originally intended to describe the interaction between the host and the parasitoid. The model took the derivatives of a sigmoid in arctan function to show the slope of a sigmoid in any given pair was done by tangents and normalized the output to one during training. Lastly, we have a stability analysis of the system: to comma and an R locus for the fixed points by the Jacobian matrix eigenvalues of the model have been given, so the type behavior of this model is described. Also, domestication is the chaos for this model: a 2D controlled low can stabilize a given system. We presented a new concept of applying the HPM system as the activation function in AI binary medical image classification: SPECT Heart data. HPM system outperforms the traditional sigmoid function extensively which can improve the accuracy and quality of image classification within and outside the applicability spectrum.

## 1. INTRODUCTION

The dynamical systems are increasingly utilized in modeling biological and ecological systems [1-4]. A new model called the Host-Parasitoid Model (HPM) combines the above two theories and has succeeded in simulating populations of phytophagous insects. The HPM differs from the above 2D systems in that it includes an activation function motivated by how artificial neural networks are used in intelligence-based tasks [5, 6].

The system Host-Parasitoid Model can be utilized to portray changes in the population of both the host and parasitoid species across discrete time intervals [7].

The basis of this model comprises a set of equations that demonstrate the changes in population for both species over time. Dye [8] introduced the population system given by the following equation:

$$P(t + \alpha) = \frac{\sigma P(\alpha)}{(1 + \varphi P(\alpha))^\mu} \quad (1)$$

where,  $P(\alpha)$ ,  $P(t+\alpha)$  refer to the population magnitudes in groups. The parameter  $\sigma$  represents the rate of growth which takes into account fertility after accounting for the lifetime density of autonomous humanities. We also introduce  $\varphi$  to

represent water containers and  $\mu$  to denote the slope of the association, between humanity and log population size. This model was formulated by May [9] and as follows:

$$P(t + \alpha) = \sigma(P(\alpha)) \exp(-\varphi P(\alpha)) \quad (2)$$

Another design has been presented by Bellows [10] as follows:

$$P(t + \alpha) = (\sigma P(\alpha)) \exp(-\varphi P^\mu(\alpha)) \quad (3)$$

The Eqs. (1)-(3) are generalized as a 2D-system, it is called the parasitoid-host system (PHS) [11], as follows:

$$\begin{aligned} H(t + \alpha) &= (\sigma_1 H(\alpha))(F(P(\alpha), H(\alpha))) \\ P(t + \alpha) &= (\sigma_2 H(\alpha))(1 - F(P(\alpha), H(\alpha))) \end{aligned} \quad (4)$$

• Here  $H$ ,  $P$  represent the population densities of the host and parasitoid.

•  $F: \mathbb{R}_+ \times \mathbb{R}_+ \rightarrow \mathbb{R}_+$  one of the Eqs. (1)-(3) indicates the fraction of the host population that is not infected.

It follows that:  $F(P(\alpha), H(\alpha)) = \exp(-\varphi P^\mu)$  and  $F(P(\alpha), H(\alpha)) = (1 + \varphi P(\alpha))^{-\mu}$ .

The logistic map is obtained when  $\mu=1$ , such that  $F(P(\alpha), H(\alpha)) = (1 + \varphi P(\alpha))^{-1}$ .

By simple calculation we have  $F(P(\alpha), H(\alpha)) = \exp(-\varphi P^\alpha)$  [8].

In this study, the tangent inverse is proposed to represent the shifted and scaled type of the logistic map  $F(P(\alpha), H(\alpha)) = \tan^{-1}(P(\alpha))$ . It is labelled as an activation and a Sigmoid function (utility function). In terms of applications, it can be used in artificial neural networks.

- $\sigma_1$  refers to the growth of the host size;
- $\sigma_2$  refers to the parasitoid population rate;
- $\alpha, t$  represents the time and iteration respectively.

Crops and its pests could be described by using the HPM. Various factors affecting interactions, such as pesticides or changes due to the external environment, are also considered. In this model, the “host” is the crop population, and the “parasitoid” is a pest acting on the given crops. The HPM is an offer to embrace a model of the complex relationship between crops and pests in agriculture. The influences are harder to predict and model but also allow modeling of the various factors influencing a system: pest control and nutrient availability, allowing a fuller picture. Several case studies seem to investigate the method for system consideration. In terms, Din [12] described the global dynamics for the proposed model and modified the model PHS, introducing the retreat effects as constant. Salih et al. [13] took into consideration chaos control and Neimark-Sacker bifurcation and the PHS was modified using a growth function for the host population. A class of PHS was approved by Hopf bifurcation and global stability conducted by Al-Saidi et al. [14]. The 3D-chaotic discrete system of vector-borne diseases that uses deep analysis and the environment component has been proposed by Salih and Al-Saidi [15] and Hussain et al. [16].

As the traditional and nonlinear dynamics used to study the interaction between host and parasitoid do not accurately figure the complex nature of this interaction, the need for high nonlinearity emerged as one of the requirements to understand many natural phenomena. Besides, some of such system is based on discrete time intervals, which resulted in an inaccurate prediction of the dynamics of this biological system. Moreover, the high sensitivity in some traditional models makes them unpreferable to be applied in real-world situations, especially when the parameters are not known. All of such limitations can be addressed in this work by introducing an advanced mathematical model inspired by the artificial neural networks that are based on the proposed nonlinear function as an activation function. This advanced approach can provide more accurate results and broaden the model's applicability in real-world applications.

In this study, we introduced a new Host Parasitoids Model (HPM) to show the intricate relationship in dynamical systems theory that aims to understand the dynamics between hosts and their parasitoids. Unlike the 2D systems, the HPM incorporates an activation function that draws inspiration from how artificial neural networks are employed in intelligence-based tasks. The rationale behind choosing the arctan activation function is due to several reasons, such as:

1. It is non-linearity and sigmoidal nature, which is an important property to model a non-linear dynamic in NN that helps in good prediction capability.
2. Its symmetrical nature of the origin helps in providing the balance to positive and negative inputs to be treated uniformly.
3. The smoothness of its derivative, which does not give sharp change or discontinuities makes it important for training algorithms like backpropagation to ensure a stable gradient descent process.

## 2. THE DESCRIPTION OF THE PROPOSED MODEL

In this section, we provide examples of several systems that are pertinent to System (4). The following structure is treated as follows:

$$\begin{aligned} H_{n+1} &= (\sigma_1 H_n)(F(P_n, H_n)) \\ P_{n+1} &= (\sigma_2 H_n)(1 - F(P_n, H_n)) \end{aligned} \quad (5)$$

If  $F(P_n, H_n) = \tan^{-1}(P_n)$  then:

$$\begin{aligned} H_{n+1} &= (\sigma_1 H_n)(\tan^{-1}(P_n)) \\ P_{n+1} &= (\sigma_2 H_n)(1 - \tan^{-1}(P_n)) \end{aligned} \quad (6)$$

The  $\tan^{-1}(\cdot)$  is used as an activation function in artificial neural networks. As a result, we can determine the sigmoid arc's slope at every two points. The resulting values take a range between [0, 1] by normalizing the output of every point. Also,  $\tan^{-1}(\cdot)$  has a symmetric value in [-1, 1].

Furthermore, it is possible to extend Model (6) by utilizing the operator of differentiation.

$$\delta(X_n) = X_{n+1} - X_n$$

To formulate the model:

$$\begin{aligned} H_{n+1} - H_n &= (\sigma_1 H_n)(\tan^{-1}(P_n)) - H_n \\ P_{n+1} - P_n &= (\sigma_2 H_n)(1 - \tan^{-1}(P_n)) - P_n \end{aligned} \quad (7)$$

This implies the model:

$$\begin{aligned} \delta(H_n) &= (\sigma_1 H_n)(\tan^{-1}(P_n)) - H_n \\ \delta(P_n) &= (\sigma_2 H_n)(1 - \tan^{-1}(P_n)) - P_n \end{aligned} \quad (8)$$

## 3. STABILITY ANALYSIS AROUND THE FIXED POINTS

Stability analysis of fixed points is also examined in this section. Using a Jacobian matrix analysis. Given is the Jacobian matrix of Model (8).

$$J = \begin{pmatrix} \frac{\partial f_1}{\partial H} & \frac{\partial f_1}{\partial P} \\ \frac{\partial f_2}{\partial H} & \frac{\partial f_2}{\partial P} \end{pmatrix} = \begin{pmatrix} \sigma_1 \tan^{-1}(P) - 1 & \frac{\sigma_1 H}{P^2 + 1} \\ \sigma_2 (1 - \tan^{-1}(P)) & \frac{-\sigma_2 H}{P^2 + 1} - 1 \end{pmatrix}$$

where,  $\begin{pmatrix} f_1(H, P) \\ f_2(H, P) \end{pmatrix} = \begin{pmatrix} (\sigma_1 H)(\tan^{-1}(P)) - H \\ (\sigma_2 H)(1 - \tan^{-1}(P)) - P \end{pmatrix}$ .

A simple calculation show that Model (8) has two fixed points namely these are:

1.  $E_0 (0,0)$  is always exist;
2.  $E_1 (H^*, P^*)$ .

### 3.1 Local stability of $E_0$

The  $J_{E_0}$  become  $J_{E_0} = \begin{pmatrix} -1 & 0 \\ \sigma_2 & -1 \end{pmatrix}$ .

Then the eigenvalues of  $J_{E_0}$  are  $\lambda_{1,2} = -1$ . Hence,  $E_0$  is asymptotically stable.

### 3.2 Local Stability of $E_1 (H^*, P^*)$

The  $J_{E_1}$  become:

$$J_{E_1} = \begin{pmatrix} \frac{\partial f_1}{\partial H} & \frac{\partial f_1}{\partial P} \\ \frac{\partial f_2}{\partial H} & \frac{\partial f_2}{\partial P} \end{pmatrix} = \begin{pmatrix} \sigma_1 \tan^{-1}(P^*) - 1 & \frac{\sigma_1 H^*}{p^{*2}+1} \\ \sigma_2(1 - \tan^{-1}(P^*)) & \frac{-\sigma_2 H^*}{p^{*2}+1} - 1 \end{pmatrix}.$$

Then the eigenvalues of  $J_{E_1}$  are  $\lambda_1 = \frac{2\sigma_1 \tan\left[\frac{2}{\sigma_1}\right]}{(-2+\sigma_1)\sigma_2}$  and  $\lambda_2 = \tan\left[\frac{2}{\sigma_1}\right]$ .

Regarding the unique fixed point  $E_1$  we get:

1.  $E_1$  is sink (stable) if  $\sigma_1=5, \sigma_2=4$ .
2.  $E_1$  is source (unstable) if  $\sigma_1=1.1, \sigma_2=1.3$ .
3.  $E_1$  is saddle point if  $\sigma_1=\sigma_2=1$ .

### 3.3 Global stability

**Definition:** (Global Stability of Steady-State Equilibriums)

A steady-state equilibrium,  $x$ , of the difference equation  $x_{n+1}=ax_n$  is globally (asymptotically) stable, if  $\lim_{n \rightarrow \infty} x_{n+1} = \bar{x} \forall x_0 \in \mathcal{R}$ .

#### 3.3.1 Global stability of $E_0$

The  $J_{E_0}$  transform into  $J_{E_0} = \begin{pmatrix} -1 & 0 \\ \sigma_2 & -1 \end{pmatrix}$ .

Next, the eigenvalues of  $J_{E_0}$  are  $\lambda_{1,2}=-1$ , hence  $E_0$  is global asymptotically stable.

#### 3.3.2 Global stability of $E_1(H^*, P^*)$

The  $J_{E_1}$  become:

$$J_{E_1} = \begin{pmatrix} \frac{\partial f_1}{\partial H} & \frac{\partial f_1}{\partial P} \\ \frac{\partial f_2}{\partial H} & \frac{\partial f_2}{\partial P} \end{pmatrix} = \begin{pmatrix} \sigma_1 \tan^{-1}(P^*) - 1 & \frac{\sigma_1 H^*}{p^{*2}+1} \\ \sigma_2(1 - \tan^{-1}(P^*)) & \frac{-\sigma_2 H^*}{p^{*2}+1} - 1 \end{pmatrix}.$$

Accordingly, the eigenvalues of  $J_{E_1}$  are  $\lambda_1 = \frac{2\sigma_1 \tan\left[\frac{2}{\sigma_1}\right]}{(-2+\sigma_1)\sigma_2}$  and  $\lambda_2 = \tan\left[\frac{2}{\sigma_1}\right]$ , then  $E_1$  is global asymptotically stable if  $\sigma_1=1.5, \sigma_2=1.5$ .

### 3.4 Ecological significance based on stability analysis

To explain the above result in the context of ecological dynamics. This method helps clarify the underlying mathematics by making connections with ecological knowledge, which can be used to understand the behavior of the ecosystems. However, based on the Jacobian matrix, the behavior of the fixed points can be interpreted as follows:

- If the fixed point (0,0) is stable (asymptotically). It suggests that both populations may eventually go extinct if no action is taken. This could happen in situations where there is a high death rate or low fertility, indicating that conservation efforts might be necessary to keep the species from going extinct.

- Local stability of  $E_1$  (Coexistence State): The stability of both species at a non-trivial fixed point  $E_1(H^*, P^*)$  indicates a balanced ecological interaction in which neither species significantly outcompetes the other.

- The analysis demonstrates how the growth rate parameters ( $\sigma_1$ ) and ( $\sigma_2$ ) affect the stability of the system. To stabilize the populations, this sensitivity can direct the adjustment of these parameters through ecological practices like controlled breeding programs or habitat manipulation. By providing ecological interpretations to stability analysis, we can truly

understand this theoretical model and bridge the gap between it and real-world ecological management. It becomes possible for the ecologist or conservator to take these understandings with him practically, resulting in more well-informed and, hence, successful management choices that help to achieve the goals of pest control and conservation alike.

### 3.5 Bifurcations analysis

The parameter whose value affects the behavior of the system is called the bifurcation. A diagram that shows how the dynamic changes are used to describe this phenomenon. Figure 1 displays the bifurcation diagram for Model (8). While Figure 2 depicts the behavior of this model for different values of  $\sigma$ .

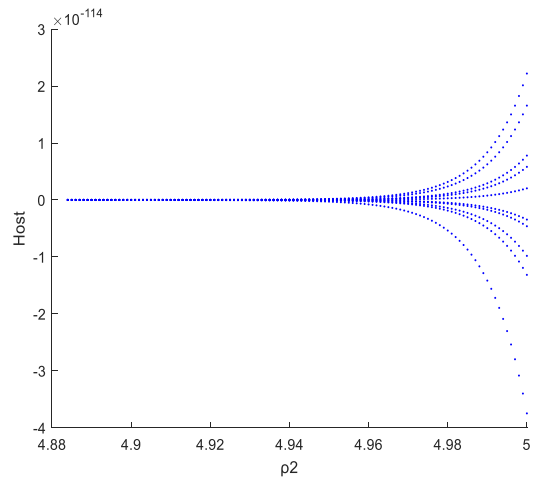


**Figure 1.** Bifurcation diagram of the Host-Parasitoid

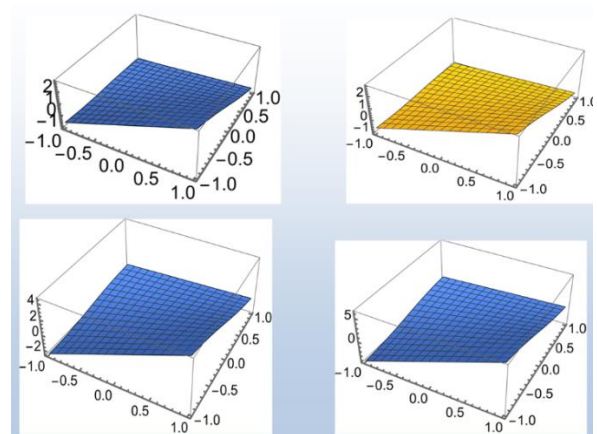


**Figure 2.** Model (8) when  $\sigma_1=2, \sigma_2=[0.75, 1, 2, 3]$

### 3.6 Lyapunov exponent (LE)

The nonlinear dynamical systems are basically chaotic, as evidenced by their great sensitivity to the initial state. Let us assume an exponential divergence between two neighbouring trajectories of a dynamical system. The Lyapunov exponent, a chaotic system, is then described through this arbitrary invariant in that scenario. According to Figure 3, the LE looks at the chaosity of Mode (8). In some parameters, it demonstrates that the suggested system exhibits chaotic behavior. When defining the local instability of a system, the average of LE is utilized.

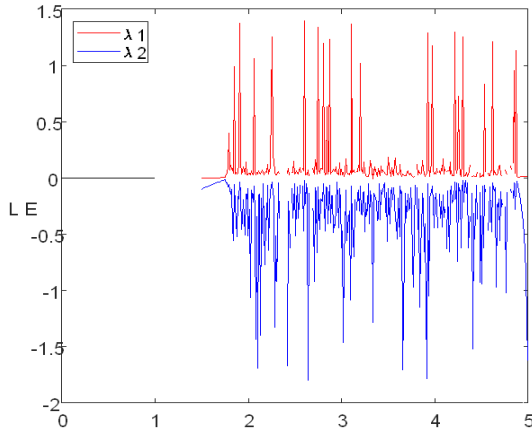


**Figure 3.** Lyapunov exponent of the Host-Parasitoid

#### 4. CONTROL OF CHAOS IN MODEL (8)

The 2D-controller law can be applied to Model (8) in the following manner:

$$\begin{aligned} U_H &= -(\sigma_1 H)(\tan^{-1}(P_n)) \\ U_P &= -(\sigma_2 H)(1 - \tan^{-1}(P_n)) \end{aligned} \quad (9)$$

Theorem: The 2D-controller (9) can be used to control the Model (8).

Proof: The following is how to identify the controlled model:

$$\begin{aligned} \delta(H) &= (\sigma_1 H)(\tan^{-1}(P)) - H - U_H \\ \delta(P) &= (\sigma_2 H)(1 - \tan^{-1}(P)) - P - U_P \end{aligned} \quad (10)$$

By changing (9) with (10), we get:

$$\begin{aligned} \delta(H) &= -H \\ \delta(P) &= -P \end{aligned} \quad (11)$$

As a matrix form, we have:

$$\begin{pmatrix} \delta(H) \\ \delta(P) \end{pmatrix} = \begin{pmatrix} -1 & 0 \\ 0 & -1 \end{pmatrix} \begin{pmatrix} H \\ P \end{pmatrix} \quad (12)$$

The goal is to show that Eq. (11)'s equilibrium is asymptotically stable, meaning that as time goes on, the model states converge to zero. Since the model's eigenvalues  $\lambda_{1,2} = -1$  are all negative, the system is stabilized since the zero outcome is asymptotically stable according to the stability theorem.

**Theorem 1:** Let  $\Lambda = \{\tau_1, \tau_2, \dots, \tau_n\}$  be an arbitrary set of  $n$  complex numbers such that  $\bar{\Lambda} = \{\bar{\tau}_1, \bar{\tau}_2, \dots, \bar{\tau}_n\} = \Lambda$ . Then the pair  $\{A, B\}$  is completely controllable if and only if there exists a matrix  $K$  such that the eigenvalues of  $A - BK$  are the set  $\Lambda$ .

We can write the system (10) in the following form:

$$\begin{bmatrix} x_{(n+1)} \\ y_{(n+1)} \end{bmatrix} = A \begin{bmatrix} x_n \\ y_n \end{bmatrix} + B \begin{bmatrix} U_x \\ U_y \end{bmatrix}.$$

It can be linearized as follows:

$$A = \begin{bmatrix} \frac{\partial f_1}{\partial x_1} & \dots & \frac{\partial f_1}{\partial x_n} \\ \vdots & \ddots & \vdots \\ \frac{\partial f_n}{\partial x_1} & \dots & \frac{\partial f_n}{\partial x_n} \end{bmatrix}, B = \begin{bmatrix} \frac{\partial f_1}{\partial u_1} & \dots & \frac{\partial f_1}{\partial u_n} \\ \vdots & \ddots & \vdots \\ \frac{\partial f_n}{\partial u_1} & \dots & \frac{\partial f_n}{\partial u_n} \end{bmatrix}.$$

Let,  $A \in R^{n \times n}$ ,  $B \in R^{n \times m}$  choose  $u \in R^{m \times n}$ .

Lemma 1: if the pair  $\{A, B\}$  is completely controllable and the column of  $B$  ( $b_1, b_2, \dots, b_n$ ) are assumed to be nonzero, then there exist matrices  $U_i$ ,  $1 \leq i \leq n$ , such that the pair  $\{A - BU_i, b_i\}$  are completely controllable, where,

$$\begin{aligned} A &= \begin{bmatrix} (\sigma_1 H)(\tan^{-1}(P)) & -H \\ (\sigma_2 H)(1 - \tan^{-1}(P)) & -P \end{bmatrix}, \\ B &= \begin{bmatrix} -(\sigma_1 H)(\tan^{-1}(P)) \\ -(\sigma_2 H)(1 - \tan^{-1}(P)) \end{bmatrix}. \end{aligned}$$

Then  $\text{Rank}(BAB) = n$ , and  $\text{Rank}(A - BU_i, b_i) = n$ .

Note that  $\{b_1, b_2\}$  represents the desired eigenvalues for the completely controllable pair  $\{A, B\}$ .

Because the control method uses terms (like  $\tan^{-1}$ ) that are directly derived from the model's equations, it preserves the system's non-linear characteristics and natural dynamics. This procedure ensures that the control inputs are both mathematically and ecologically compatible. This obviously is shown in Figure 4.

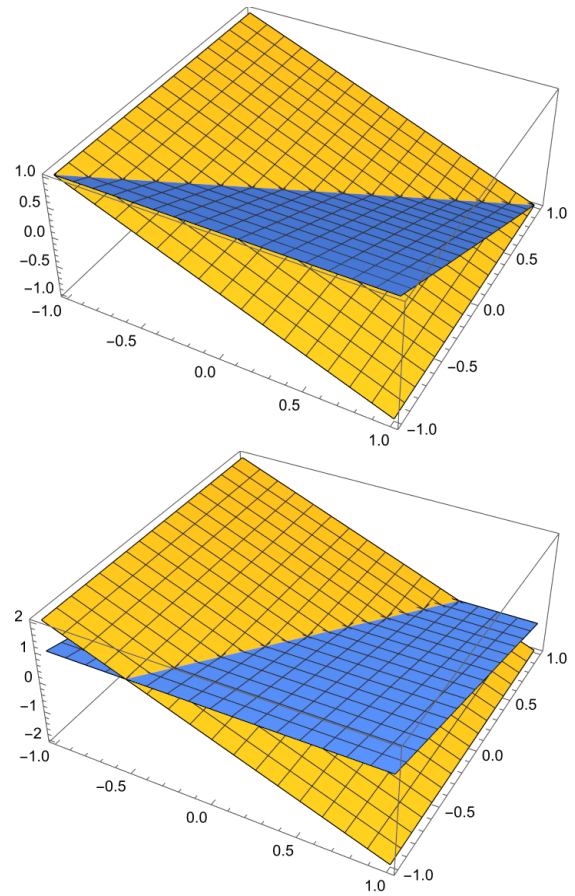


**Figure 4.** Model (8) after control, for  $\sigma_1=1$ ,  $\sigma_2=[1, 2]$

Eqs. (9)-(10) explain how the stabilization is achieved.

The control strategy seeks to achieve an asymptotically stable equilibrium in which, independent of initial conditions, the populations of parasitoids and hosts eventually converge to the fixed points. The method avoids extreme scenarios that could have disastrous ecological effects, like the host going extinct or the parasitoid spreading unchecked. Instead, it controls chaos within the system. Therefore, the Host-Parasitoid Model's 2D control law for chaos control was selected because it is straightforward, efficient, and consistent with the dynamics of the system. In doing so, this approach

improves the predictability and manageability of host-parasite interactions by directly integrating with the model's equations to achieve stabilization and provide a strong mechanism to guide the system towards desired ecological states.

## 5. DISCUSSION

The Host-Parasitoid Model is described in this manuscript. First, a few qualitative aspects of the host-parasite model are talked about. The stability of the fixed points and their existence are examples of these characteristics. Furthermore, it is demonstrated that Model (8) experiences a Neimark-Sacker bifurcation around a fixed point and computation the maximal Lyapunov exponents. Furthermore, the proposed models' chaotic behavior is managed through the application of chaos control methodology. It is observed that the host and parasite model presented in Figure 3 exhibits chaos as the value of  $\sigma_2$  increases, indicating that the parasite outpaces the host in terms of growth rate and eventually restores stability to the system through the use of the control mechanism and as seen in the ensuing Figures 5 and 6.

Although the model might work well in controlled or particular environments, there may be limitations to its scalability to larger, more complex ecosystems or its applicability to other ecological contexts. A two-species model may not adequately capture the complexity of interactions found in diverse ecosystems. Overfitting to the training data is a constant risk associated with complex models. This may reduce the model's general utility by making it less predictive when used with fresh data or under different circumstances.

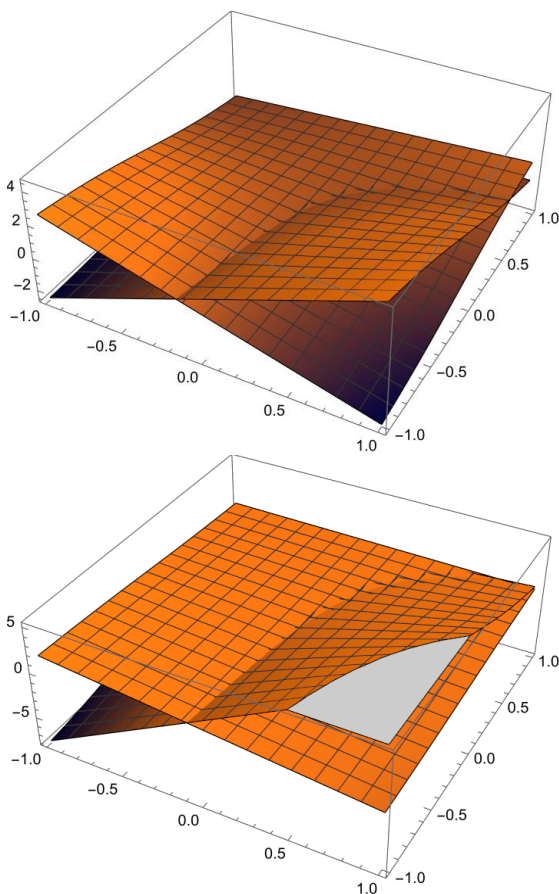


**Figure 5.** Model (8) before control, for  $\sigma_1=1$ ,  $\sigma_2=[1, 2]$

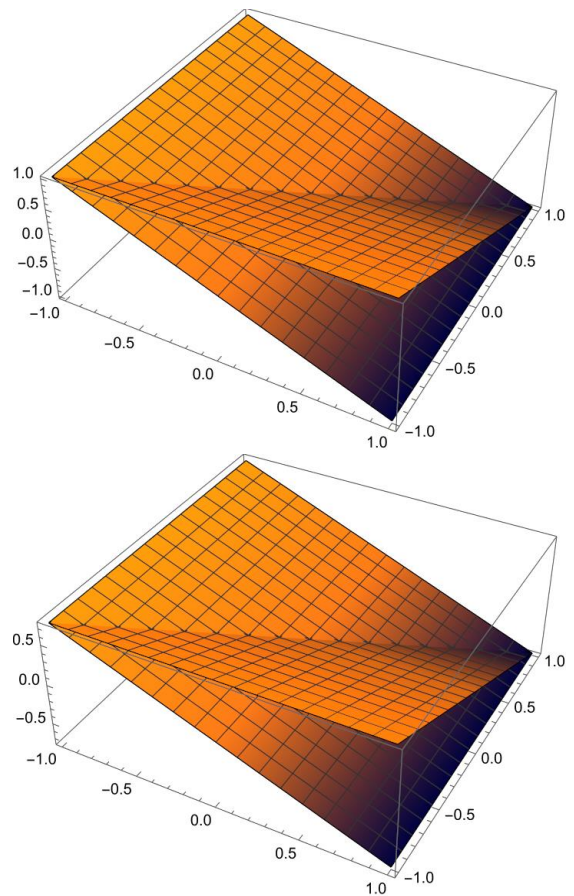


**Figure 6.** Model (8) after control, for  $\sigma_1=1$ ,  $\sigma_2=[1, 2]$

## 6. THE IMPACT OF HPM IN AI

The hyperbolic tangent function in the HPM model is well suited for use as an activation function in neural networks. It helps normalize neuron outputs, facilitating training and improving convergence rates. In learning, such functions introduce non-linearity to the model, enabling the network to learn intricate patterns and make more accurate predictions.

For example, the hyperbolic tangent function in Eq. (6):

$$\begin{aligned} H_{n+1} &= (\sigma_1 H_n) (\tan^{-1}(P_n)) \\ P_{n+1} &= (\sigma_2 H_n) (1 - \tan^{-1}(P_n)) \end{aligned}$$

is a sigmoidal (S-shaped) curve spanning from -1 to 1. When used as an activation function, the  $\tan^{-1}(x)$  normalization device centres data at zero which is a great advantage for networks of this type. It helps to reduce variance between layers and stave off collapse during backpropagation. This specific feature was utilized as early as 1986 by Rumelhart and McClelland [17]. As a result, many important network training algorithms have been widely adopted today.

### 6.1 Application of the proposed model in artificial intelligence

By using mathematical techniques, we not only enhance our understanding of natural phenomena but also establish a strong framework for addressing complex challenges in the ever-changing and evolving world of artificial intelligence. As we continue to explore the connections between these fields, the potential for solutions and transformative impacts becomes

increasingly clear. As for the Host-Parasitoid Model, its hyperbolic tangent function has been used in different AI applications for the same ability to effectively model complex dynamics. Some of these applications include:

- Environmental management and protection (conservation). Using the HPM, one Autonomous Artificial Animal (A3) can fare well across vast regions. To forecast ecosystem changes a year from now based on environmental policy choices or other macro-run decisions; and so on with ever more timely accuracy! For example, neural networks can be trained to anticipate the consequences of introducing a new species or an approach to conservation.
- Ecological Conservation and Management: The HPM can be used in AI systems to predict what will happen when different conservation strategies are tried out.
- Image Classification in Ecology: The HPM updated Convolutional Neural Networks (CNNs) and can now smoothly handle image classification tasks such as species recognition and the judgement of ecological changes based on satellite images.
- Public Health and Vector Control: The HPM can be adjusted to model vector-borne diseases. It is this characteristic of it that lets us forecast and then go after outbreaks through host-vector dynamics.

In this work we will focus on the medical image classification and the effect of using HPM as an activation function.

### 6.1.1 The implementation of HPM in medical image classification

The specific requirements of the implementation are: choosing one of the AI algorithms, the type of dataset, and a specific ecological conservation. For example, in this implementation, we choose the Convolution Neural Network (CNN) algorithm for the image classification task [18], and as a type of dataset, we choose medical images, with the HPM model used as an activation function for binary output prediction [19].

To incorporate the Host Parasitoid Model (HPM) into a Convolutional Neural Network (CNN), we apply the equations of the HPM to the results generated by the layers of CNN. This process can be seen as a processing stage, where we fine-tune the predictions of the CNN using the principles and concepts of the HPM.

If we suppose that the CNN generates a set of probabilities for each class (in this work 'host' and 'parasitoid') for every image. These probabilities can be denoted as  $P_{host}$  and  $P_{parasitoid}$ . Therefore, the HPM is applied to these probabilities as follows:

The basic form of the HPM is:

$$\begin{aligned} H_{new} &= (\sigma_1 H)(\tan^{-1}(P)) \\ P_{new} &= (\sigma_2 H)(1 - \tan^{-1}(P)) \end{aligned}$$

where,  $H$  and  $P$  refer to the population densities of the host and parasitoid respectively, which can be comprehended in CNN as the probabilities  $P_{host}$  and  $P_{parasitoid}$ .

After the CNN completes its predictions, we apply the HPM equations to adjust them such that:

$$\begin{aligned} P_{host,new} &= (\sigma_1 P_{host})(\tan^{-1}(P_{parasitoid})) \\ P_{parasitoid,new} &= (\sigma_2 P_{parasitoid})(1 - \tanh(P_{parasitoid})) \end{aligned}$$

The values of the parameters  $\sigma_1$  and  $\sigma_2$  can be adjusted based on requirements or obtained through the training process.

In the CNN, the input is the images, and the output is the initial predictions ( $P_{host}$  and  $P_{parasitoid}$ ), which are then fed into the HPM equations.

The output of the HPM equations is ( $P_{host,new}$  and  $P_{parasitoid,new}$ ), which represent the final adjusted predictions.

This method enables the CNN to analyze the images and generate predictions, which are later improved by incorporating the dynamics represented in the HPM. It is a strategy that combines learning's ability to recognize patterns, with the knowledge embedded in the HPM. The values of the parameters  $\rho_1$ , and  $\rho_2$  should be carefully chosen to ensure that the HPM model reflects the ecological relationship, which we aspired to obtain through the proposed model.

Now, we explore the applicability of the (HPM) serving as an activation function in the framework of a Convolutional Neural Network (CNN) for binary medical image classification. This is just posed with the typical usage of a sigmoid activation function. The motivation for the exploration is to investigate the potential impact of HPM in the predictive accuracy and efficiency of the system. The dataset utilized in this study is the SPECT Heart data, comprising 267 patient records, each categorized as either normal or abnormal. These SPECT image sets were sourced from the Kaggle SPECT MPI dataset, which provides medical scan images similar to CT scans [20]. To facilitate the analysis, we initially extracted key features from the original SPECT images, effectively summarizing the complex data into a more manageable form. To illustrate, we selected a representative image from the original dataset for both normal and abnormal cases, as depicted in Figure 7 [20]. The subsequent feature extraction process, as detailed in reference [21], yielded 44 continuous features per patient. These features were then further refined into 22 binary feature patterns, allowing for a more streamlined analysis. Importantly, our analysis focused on these extracted features, not the raw images, enabling a more efficient and targeted investigation into the distinguishing characteristics of normal versus abnormal cases.

The CNN model used consists of:

- Input Layer: The input shape is carefully chosen to best match the problem and the size of the images expected as input. In this case, the images are square and have a size 64×64 pixels with 1 color channel for greyscale. This is not explicitly an input layer; it can be considered an input layer in this model.

- Conv2D Layer: This is the first hidden layer and is a convolutional layer. It has 32 filters each with a size of 3×3. This layer will take the input image and create 32 new images, each based on the local (3×3) region of the image. The activation function is the rectified linear unit or ReLU. This function has the general form  $f(x) = \max(0,x)$ , and in this case, it will output the input directly if it is positive. Otherwise, it will output zero. The result is a very simple non-linearity.

- Flatten Layer: As its name suggests, this layer flattens the output of the Conv2D layer so that you can make use of fully connected layers. The 2D output from the previous layer becomes a 1D array.

- Dense Layer (Output Layer): A dense (also known as fully connected) layer with a single output unit and an HPM activation function is a standard output layer setup for a binary classification problem. The output value is in the range [0, 1] and can be rounded to get the predicted class value of 0 or 1.

The results are illustrated in Figures 7 and 8. In Figure 9, we first set the size of the epoch to ten as a preliminary test of what would happen. Then, at a later stage, to avoid the system being overfitting, the early stopping technique was applied, as

shown in Figure 8. Using this strategy permitted us to make adjustments for the future course of training and to check our

model's ability to generalize.

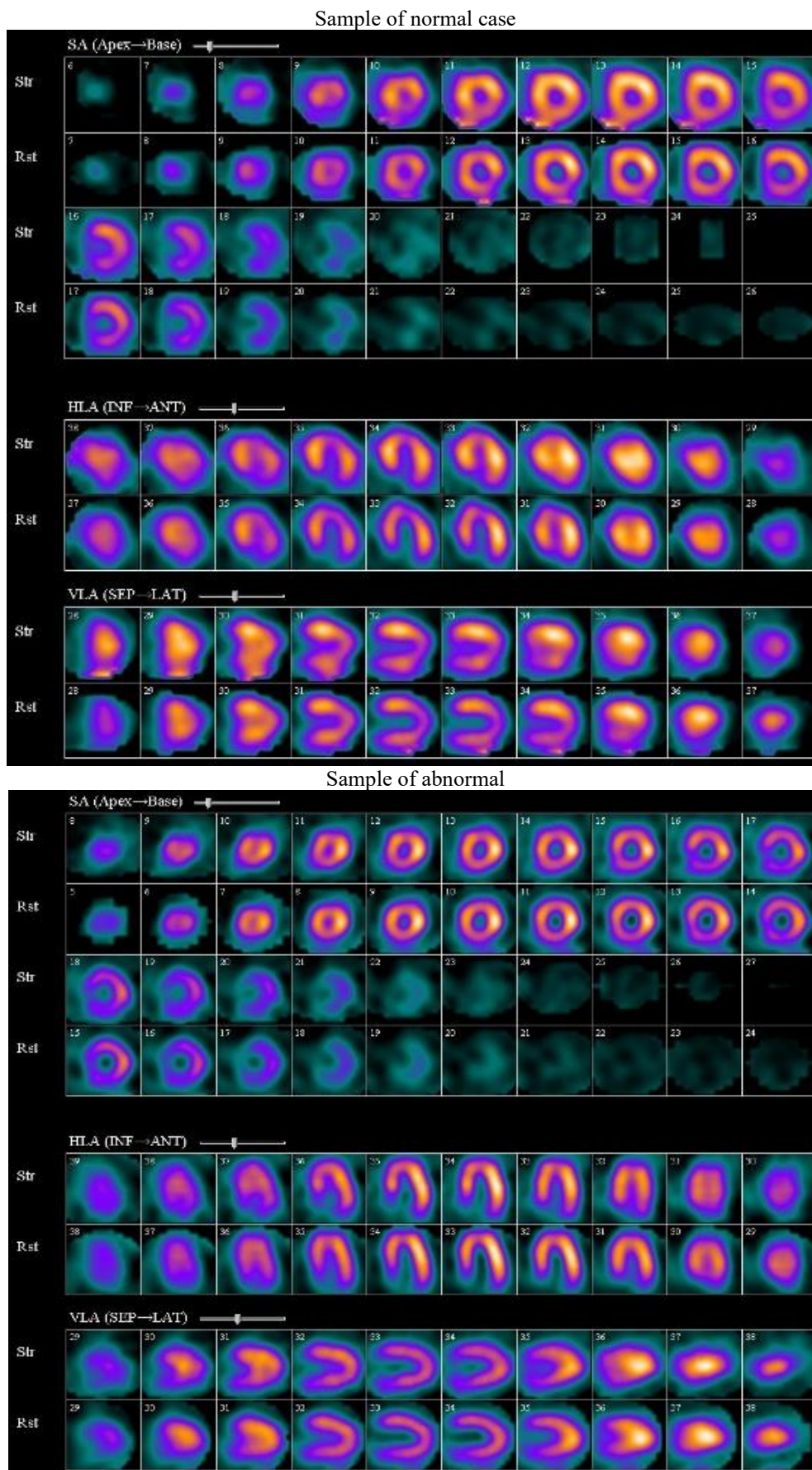


**Figure 7.** Original CT images, SPECT images dataset for normal and abnormal cases

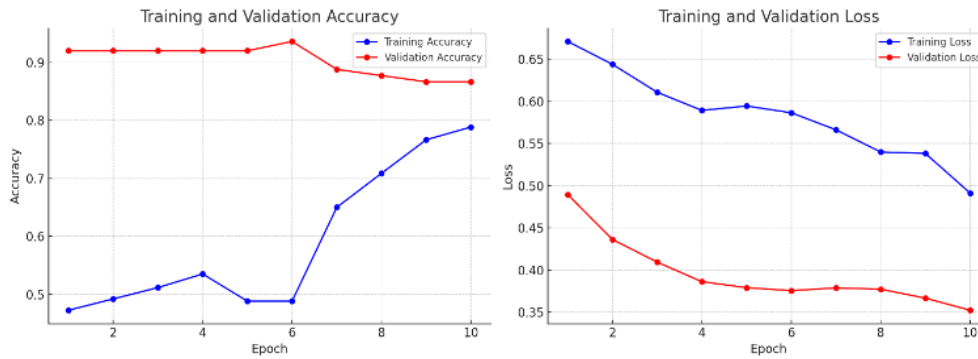


**Figure 8.** Training vs. validation accuracy and training vs. validation loss without early stopping

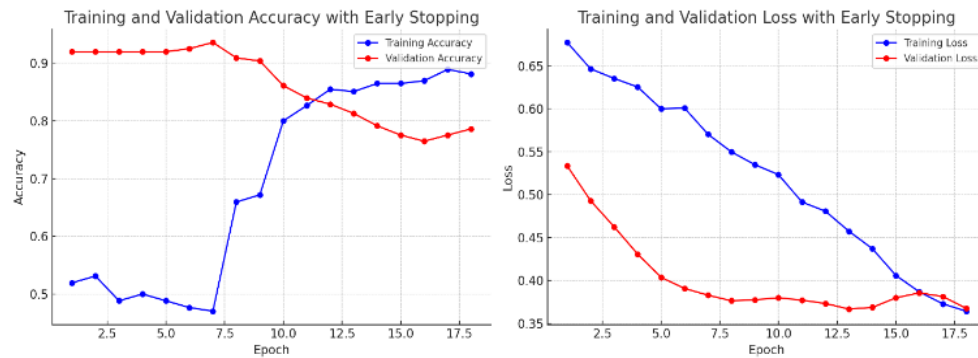


**Figure 9.** Training vs. validation accuracy and training vs. validation loss with early stopping

In Figure 8, the left graph shows the model's accuracy on the training and validation sets. The training accuracy starts high, and over time it remains at a similar level, which indicates that the model is fitting to the training data effectively over the epochs. The validation accuracy, however, increases substantially really up to about the sixth epoch and then ceases to improve. This might indicate that the model has learned the relevant patterns in the validation data by the sixth epoch, and training beyond that point does not yield improvements in accuracy. Additionally, the right graph shows the loss over the epochs, for both the training and validation sets. The training loss is decreasing throughout, and as the bottom graph shows, this demonstrates that the model is learning and getting better at making predictions based on the training data. The validation loss is decreasing in conjunction with the training loss up until the sixth epoch when the loss starts to show some volatility. It increases then decreases, across the sixth epoch. This increase in validation loss might suggest that we are starting to over-fit the model. In summary, these graphs show us the model is learning well but there is certainly a risk of over-fitting after the sixth epoch, suggested by the plateau in validation accuracy and the slight uptick in validation loss. With early stopping, the original message we saw suggests stopping training when the validation loss starts to increase and guarantees that the model will not lose its ability to generalize to unseen data, as shown in Figure 8.

In Figure 9, the left chart, which shows accuracy, demonstrates that training vision is fast and then stabilizes at a high level of accuracy- which is an indication that our model has learned well. Meanwhile, accuracy in validation receives a big boost, at some points above training accuracy. This may be because there is not a large enough data set for validation, difficulties and some techniques for regularization which are actually more effective on validation data. After about the 10th epoch, the two accuracies come into approximate alignment

and are pretty flat. This illustrates clearly that early stopping has saved us from any further overfitting by halting training when validation accuracy no longer improves. The right graph, which shows a loss, teaches that training loss declines steadily - a typical trajectory during a network's learning period. Validation loss mirrors this pattern exactly until about the 10th epoch. Thereafter, it begins to plateau and even inch upward slightly in some places. This stage is evidence that the model has arrived at its best performance on the validation set in generalization terms and that any further training above and beyond this point may not produce significant improvement.

In order to fully evaluate the performance of the HPM that is used as an activation function in our medical application, a detailed experimental study was conducted. This comprehensive approach followed K-Fold cross-validation, using  $k=5$  as a fold, to suppress the variability of our results and raise their precision significantly. Also, an early stopping method to avoid overfitting with Adam regularization Function. In this framework, the time-honoured sigmoid activation function often employed in binary classification models was pitted against the HPM activation function we propose here (likewise tailored for binary classification). Table 1 gives a nuanced comparison of these performances, providing fresh insights into our work.

**Table 1.** The accuracy results of heart SPECT dataset after applying sigmoid and HPM activation function with 5-fold

| Fold           | Sigmoid Results          | HPM Results              |
|----------------|--------------------------|--------------------------|
| Fold 1         | 96.66666388511658        | 96.66666388511658        |
| Fold 2         | 89.99999761581421        | 89.99999761581421        |
| Fold 3         | 93.33333373069763        | 93.33333373069763        |
| Fold 4         | 86.66666746139526        | 86.66666746139526        |
| Fold 5         | 89.65517282485962        | 89.65517282485962        |
| <b>Average</b> | <b>91.26436710357666</b> | <b>92.26436710357666</b> |



The inquiry is substantiated on the hypothesis that the use of HPM in the image of a CNN may result in significant improvements in the classification performance especially in the better-nuanced domain of medical imaging.

### 6.2 The chaotic behavior of HPM in AI

By utilizing the proposed HPM with its hyperbolic tangent function, AI can further explore the intersection between chaos theory and intelligent systems. The concept of chaos in the proposed model can be utilized in AI systems that operate in environments characterized by unpredictability and disorder. This is considered crucial in systems and environments where conditions change quickly and unexpectedly. The AI system is used to show how conservation efforts will affect a given ecological region. It will focus on the relationships between hosts and their parasites as well as interactions between different species. In this work we deal with the Host-Parasitoid Model (HPM), which is represented by the following sets of equations:

1. Basic Host-Parasitoid Model (Eq. (4)):

$$\begin{aligned} H(t + \alpha) &= (\sigma_1 H(\alpha))(F(P(\alpha), H(\alpha))) \\ P(t + \alpha) &= (\sigma_2 H(\alpha))(1 - F(P(\alpha), H(\alpha))) \end{aligned}$$

The aforementioned mathematical formulas can be used in the field of artificial intelligence to predict changes that may happen in the population contributing to management decision-making by considering circumstances. For instance, one could modify a neural network to forecast the results of a conservation strategy or the introduction of a species to a new habitat.

2. Chaos control and Neimark-sacker bifurcation (Eq. (6)):

$$\begin{aligned} H_{n+1} &= (\sigma_1 H_n)(\tan^{-1}(P_n)) \\ P_{n+1} &= (\sigma_2 H_n)(1 - \tan^{-1}(P_n)) \end{aligned}$$

The concept of chaos control is proposed in this model and is critical for instances where behavior becomes unstable. To this end artificial intelligence (AI) can be used in computer systems to adjust themselves for operation in changing environments as necessary.

3. Chaos control (Eq. (8)):

$$\begin{aligned} \delta(H_n) &= (\sigma_1 H_n)(\tan^{-1}(P_n)) - H_n \\ \delta(P_n) &= (\sigma_2 H_n)(1 - \tan^{-1}(P_n)) - P_n \end{aligned}$$

These equations can be used by AI systems to predict the long-term stability of ecosystems with different strategies in place. This is especially advantageous when it comes to conservation work.

4. 2D-controller law (Eqs. (9)-(12)):

$$\begin{aligned} U_H &= -(\sigma_1 H)(\tan^{-1}(P_n)) \\ U_P &= -(\sigma_2 H)(1 - \tan^{-1}(P_n)) \\ \delta(H) &= (\sigma_1 H)(\tan^{-1}(P)) - H - U_H \\ \delta(P) &= (\sigma_2 H)(1 - \tan^{-1}(P)) - P - U_P \\ \begin{pmatrix} \delta(H) \\ \delta(P) \end{pmatrix} &= \begin{pmatrix} -1 & 0 \\ 0 & -1 \end{pmatrix} \begin{pmatrix} H \\ P \end{pmatrix} \end{aligned}$$

By this set of equations is used to control the chaos in the system to ensure stability. In the implementation of AI, these equations are usually incorporated into machine learning algorithms. The AI system utilizes both real-time data to train these models enabling it to make forecasts regarding ecological outcomes. Table 2 shows the comparison between the proposed system with one of the literature works in terms of the dynamic properties and the stabilisation.

The possible applications of artificial intelligence in the proposed model mainly fall under three categories: First, time series forecasting is one of the areas in which the typical system behind the model can be stated. This system is a dynamic, recurring system, which is comparable to the recurrent systems that the machine learning algorithm is used for time-series forecasting. Deep learning, LSTM, and GRU can accept and train on historical datasets to predict future values of  $H_n$  and  $P_n$ . The prediction is essential for economic, meteorological, or energy forecasting and planning. Artificial intelligence, further, can optimize models by running an algorithm that identifies the parameters that lead to the most likely result of the real-life data. For instance, gradient descent, genetic algorithms, and Bayesian optimization, which statistically minimize the errors made from these assumptions, can be used to fine-tune the model. Second, the model is used for system identification, in which the machine learning algorithm is fed input-output data and finds the system behind differential equations. In this setting, it is of importance in fields in which systems may be highly complex or unknown to the developers, such as engineering and physics. Third, in the field of control systems, this model is used to design the controls, if the system's parameters need to be turned in real-time or during an experiment.

**Table 2.** Comparison of HPM with reference [12] using different aspects

| Aspect/Feature        | The Proposed Host-Parasitoid Model (HPM)   | Reference [12]  |
|-----------------------|--|---|
| Basic Premise         | Function activation $F(P_n, H_n)=\tan^{-1}$ .  | Function activation $F(P_n, H_n)=\tanh$ .   |
| Stability Analysis    | 1. The set of fixed points $E_0(0,0), E_1\left(\frac{\sigma_1 \ell}{\sigma_2(\sigma_1-1)}, \ell\right)$ , where $\ell := \tan\left[\frac{2}{\sigma_1}\right]$ .<br>2. The set eigenvalues $A_{E_0} = \{\lambda_1 = -1, \lambda_2 = 1\}$ , $A_{E_1} = \{\lambda_{1,2} = \mp \frac{2}{3} \tan(2)\}$ has a saddle points. | 1. The set of fixed points $\{\varphi_0(0,0,0), \varphi_1\left(\frac{\rho_1 \ell}{\rho_2(\rho_1-1)}, \ell, \frac{[\rho_2(\rho_1-1)(\alpha-1) - \alpha\rho_1] \ell}{\rho_2(\rho_1-1)(\alpha_0-1)}\right)\}$ , where $\ell := \log\left(\sqrt{\frac{\rho_1+1}{\rho_1-1}}\right)$ .<br>2. The set eigenvalues $\Lambda_{\varphi_0} = \{\lambda_1 = 1, \lambda_{2,3} = -1\}$ , $\Lambda_{\varphi_1} = \{\lambda_1 = 1, \lambda_{2,3} = 0.01\}$ has a saddle points. |
| Bifurcation Analysis  | The range bifurcation, when $\sigma_1, \sigma_2=[4.90, 5]$ .   | The range bifurcation, when $\rho_1=2, \rho_2=[1, 2]$ .   |
| Lyapunov-exponent     | The range Lyapunov-exponent, when $\sigma_1, \sigma_2=[2, 5]$ .  | The range Lyapunov-exponent, when $\rho_1=4, \rho_2=5$ .  |
| Chaos Control Methods | Controlled by 2D-controller law<br>$U_H = -(\sigma_1 H)(\tan^{-1}(P_n))$<br>$U_P = -(\sigma_2 H)(1 - \tan^{-1}(P_n))$<br>The conduct of the chaos, when $\sigma_1=\sigma_2=[2, 5]$ .   | Controlled by 2D-controller law<br>$U_H = -(\rho_1 H)(\tanh(P_n))$<br>$U_P = -(\rho_2 H)(1 - \tanh(P_n))$<br>The conduct of the chaos, when $\rho_1=4, \rho_2=5$ .  |

## 7. CONCLUSIONS

In this study, we introduced the host model that accommodated a hyperbolic tangent function. This development pushes the envelope in modelling, drawing the connection between the novel and improved tool that will help us identify and apply complex dynamics in the discrete dynamical system framework while studying Host-Parasitoid interactions. These insights benefit the field of artificial intelligence on which we used Jacobian matrix methods to examine its stability. The host model revealed capability strengths by capturing both unstable states in any ecosystem. Without challenges nonlinear relationships seen in ecological interactions, all fluctuations varied, demonstrating the potential to understand and control difficult dynamical systems. Moreover, our chaos control mechanism addressed the unpredictability and nonlinearity related to AI systems. This feature holds value in AI applications where comprehending and controlling behaviors can greatly enhance the performance and reliability of AI driven solutions. The application of our model in AI has opened up avenues for research and development in areas such, as neural network training and predictive analytics. The model's ability to work well with AI approaches, like learning, makes it an important tool for simulating situations and making informed predictions as seen in the field of ecological conservation. To conclude our Host-Parasitoid Model represents advancement in modeling. It offers perspectives and tools for researchers and practitioners in both ecology and AI. Finally, as this research, the HPM system is an effective activation function for the implementation of artificial intelligence of binary medical image classification using CNN, which should especially be used in regard to SPECT Heart. The HPM has helped us to reach a high classification accuracy of 92.6% compared to the traditional method of binary medical image classification using the sigmoid function, which reached 91.2%. Thus, establishing the great ability of HPM to improve the accuracy and credibility of medical image analysis opens significant prospects for further development of artificial intelligence-oriented diagnostic tools.

In the field of ecological modelling, the Host-Parasitoid Model with chaos control is a promising tool that provides fresh perspectives and more dependable control techniques for handling intricate biological interactions. These systems would be very helpful in dynamic environments where decisions must be made quickly and conditions change quickly. As the new direction, understanding these effects will be essential for future ecological management, as climate change has the potential to drastically change these relationships. As well as creating systems that can use the HPM to make quick predictions based on real-time data.

## REFERENCES

- [1] Al-Saidi, N.M., Yahya, H., Obaiys, S.J. (2022). Discrete dynamic model of a disease-causing organism caused by 2D-quantum tsallis entropy. *Symmetry*, 14(8): 1677. <https://doi.org/10.3390/sym14081677>
- [2] Al-Azawi, R.J., Al-Saidi, N.M., Jalab, H.A., Kahtan, H., Ibrahim, R.W. (2021). Efficient classification of COVID-19 CT scans by using q-transform model for feature extraction. *PeerJ Computer Science*, 7: e553. <https://doi.org/10.7717/peerj-cs.553>
- [3] AL-Jubouri, K.Q., Hussien, R.M., Al-Saidi, N.M. (2020). Modeling of an eco-epidemiological system involving various epidemic diseases with optimal harvesting. *Eurasian Journal of Mathematical and Computer Applications*, 8(2): 4-27. <https://doi.org/10.32523/2306-6172-2020-8-2-4-27>
- [4] Alabacy, Z.K., Salih, S.H., Khilil, S., Al-Saidi, N.M.G. (2024). Stabilizing ecosystem dynamics: The toxicity effect on an ecosystem in the presence of self-defence. *Communications in Mathematical Biology and Neuroscience*, 2024: 62. <https://doi.org/10.28919/cmbn/8575>
- [5] Scardapane, S., Van Vaerenbergh, S., Hussain, A., Uncini, A. (2018). Complex-valued neural networks with nonparametric activation functions. *IEEE Transactions on Emerging Topics in Computational Intelligence*, 4(2): 140-150. <https://doi.org/10.1109/TETCI.2018.2872600>
- [6] Tan, Z.H., Xie, Y., Jiang, Y., Zhou, Z.H. (2022). Real-valued backpropagation is unsuitable for complex-valued neural networks. *Advances in Neural Information Processing Systems*, 35: 34052-34063.
- [7] Bellows, T.S., Hassell, M.P. (1988). The dynamics of age-structured host-parasitoid interactions. *The Journal of Animal Ecology*, 259-268. <https://doi.org/10.2307/4777>
- [8] Dye, C. (1984). Models for the population dynamics of the yellow fever mosquito, *Aedes aegypti*. *The Journal of Animal Ecology*, 247-268. <https://doi.org/10.2307/4355>
- [9] May, R.M. (1974). Biological populations with nonoverlapping generations: Stable points, stable cycles, and chaos. *Science*, 186(4164): 645-647. <https://doi.org/10.1126/science.186.4164.645>
- [10] Bellows, T.S. (1981). The descriptive properties of some models for density dependence. *The Journal of Animal Ecology*, 139-156. <https://doi.org/10.2307/4037>
- [11] Jones, T.H., Hassell, M.P., Pacala, S.W. (1993). Spatial heterogeneity and the population dynamics of a host-Parasitoid System. *Journal of Animal Ecology*, 62(2): 251-262. <https://doi.org/10.2307/3545981>
- [12] Din, Q. (2016). Global behavior of a Host-Parasitoid Model under the constant refuge effect. *Applied Mathematical Modelling*, 40(4): 2815-2826. <https://doi.org/10.1016/j.apm.2015.09.012>
- [13] Salih, S.H., Al-Saidi, N., Zboon, R.A. (2022). A reliable numerical algorithm for stabilizing of the 2-dimensional logistic hyperchaotic trajectory. *Al-Mustansiriyah Journal of Science*, 33(1): 51-56. <https://doi.org/10.23851/mjs.v33i1.1048>
- [14] Al-Saidi, N.M., Salih, S.H. (2022). A new convex controller for stabilizing of two symmetrical logistic maps. In *Journal of Physics: Conference Series*, 2322(1): 012054. <https://doi.org/10.1088/1742-6596/2322/1/012054>
- [15] Salih, S.H., Al-Saidi, N.M. (2022). 3D-Chaotic discrete system of vector borne diseases using environment factor with deep analysis. *AIMS Mathematics*, 7(3): 3972-3987. <https://doi.org/10.3934/math.2022219>
- [16] Hussain, S., Al-Saidi, N., Obaiys, S., Karaca, Y. (2024). 3D chaotic nonlinear dynamic population-growing mathematical system modeling with multiple controllers. *Chaos Theory and Applications*, 6(3): 218-227. <https://doi.org/10.51537/chaos.1446633>
- [17] Rumelhart, D.E., McClelland, J.L. (1986). Explorations in the microstructure of cognition: Foundations. In

- Parallel Distributed Processing, MIT Press.  
<https://doi.org/10.7551/mitpress/5236.001.0001>
- [18] Danovski, K., Soriano, M.C., Lucas, L. (2024). Dynamical stability and chaos in artificial neural network trajectories along training. *Frontiers in Complex Systems*, 2: 1367957. <https://doi.org/10.3389/fcpxs.2024.1367957>
- [19] Xiao, M.X., Li, Y.F., Yan, X., Gao, M., Wang, W.M. (2024). Convolutional neural network classification of cancer cytopathology images: Taking breast cancer as an example. In *Proceedings of the 2024 7th International Conference on Machine Vision and Applications*, New York, USA, pp. 145-149. <https://doi.org/10.1145/3653946.3653968>
- [20] Kaplan Berkaya, S., Ak Sivriköz, I., Gunal, S. (2020). Classification models for SPECT myocardial perfusion imaging. *Computers in Biology and Medicine*, 123: 103893. <https://doi.org/10.1016/j.compbiomed.2020.103893>
- [21] Cios, K., Kurgan, L., Goodenay, L. (2001). SPECT Heart. UCI Machine Learning Repository. <https://doi.org/10.24432/C5P304>.